ISSN 1062-8738, Bulletin of the Russian Academy of Sciences: Physics, 2017, Vol. 81, No. 7, pp. 874–878. © Allerton Press, Inc., 2017.
Original Russian Text © I.L. Romashkina, M.G. Kozin, V.P. Koshelets, L.V. Filippenko, 2017, published in Izvestiya Rossiiskoi Akademii Nauk, Seriya Fizicheskaya, 2017, Vol. 81, No. 7, pp. 966–970.

Registering the Radiation Spectrum of a Mössbauer ^{119m}Sn Source Using Superconducting Tunnel Junction Detectors

I. L. Romashkina[a], *, M. G. Kozin[a], V. P. Koshelets[b], and L. V. Filippenko[b]

[a] *Skobeltsyn Institute of Nuclear Physics, Moscow State University, Moscow, 119991 Russia*

[b] *Kotel'nikov Institute of Radio Engineering and Electronics, Russian Academy of Sciences, Moscow, 125009 Russia*

**e-mail: irom@srd.sinp.msu.ru*

Abstract—Radiation spectra from a ^{119m}Sn Mössbauer source are registered using Nb-based superconducting tunnel junction detectors. Mössbauer and accompanying X-ray radiation are detected via escape peaks with high energy resolution.

DOI: 10.3103/S1062873817070231

INTRODUCTION

For quite some time we have been studying the physics of the operation of detectors based on superconducting tunnel junctions (STJ detectors, or simply tunnel detectors) [1]. The current motivation behind our work is a desire to use STJ detectors in Mössbauer spectroscopy, and conversely to use Mössbauer methodology to study the operation of STJ detectors [2–4].

Since STJ detectors are small thin film devices, they will most likely be used in Mössbauer scattering experiments with the registration of conversion electrons. Even more interesting is that tunnel detectors have not been used so far to register electrons, although the principle of their operation during the registration of electromagnetic radiation is based on the photoelectric effect (i.e., the conversion of photon energy into photoelectron energy, with the subsequent cascade reduction of the energy in the electron–phonon system of the detector's absorber material).

Among the numerous approaches of electron Mössbauer spectroscopy [5, 6], there are two that can be used to register Mössbauer electrons at very low (helium and sub-helium) temperatures, and can be compared to the potential abilities of low-temperature tunnel detectors. The first approach is reflected in a series of works by Japanese authors from the University of Kyoto with helium-filled proportional counters (see, e.g., [7]). Another approach, in which the phenomenon of secondary electron emission is used to amplify an electronic signal in devices called channeltrons, was developed in a series of works by Savitsky with co-workers [8]).

We demonstrated the possibility of registering FeK_α and K_β X-rays, 14.4 keV γ-rays from a ^{57}Co(Rh) source [9], and the conversion electrons produced upon irradiating a RhFe resonant scatterer with this source [3, 4], using STJ detectors based on niobium. The next task is to register the electrons produced upon relaxation of the 23.8 keV state in a thin $CaSnO_3$ absorber excited by a ^{119m}Sn source (in the same $CaSnO_3$ matrix) fixed relative to the absorber. A full identification of all lines in the resulting spectrum has in this case yet to be achieved, but unexpected results have been obtained. STJ detectors registered escape peaks from niobium in the amplitude spectrum of the ^{119m}Sn Mössbauer source.

EXPERIMENTAL

The aim of this work was to register the amplitude spectra of a ^{119m}Sn Mössbauer source using superconducting tunnel detectors. The source and the chip with the detectors were placed in a low-temperature chamber in close proximity to each other.

A ^{119m}Sn Mössbauer source in a $CaSnO_3$ matrix with an active spot 15 mm in diameter and an activity of 2.5 mCi was used in our experiments. A standard ^{55}Fe source for testing detectors in soft X-rays with an active spot having a diameter of 3 mm and an activity of 0.73 mCi was used for energy calibration. $CaSnO_3$ powder enriched with ^{119}Sn isotope was deposited on a beryllium foil ~0.1 mm thick and served as a scatterer. The scatterer was 12 mm in diameter. The Mössbauer effect, recorded using an argon proportional counter, was about 10% in the absorption experiment. Using this scatterer, we were able to observe the Mössbauer effect at zero relative velocity of the source and detector.

The same silicon chip with detectors as in [3, 4] was used. The photo and the electron microscope view of the chip are shown in [4], and the current voltage

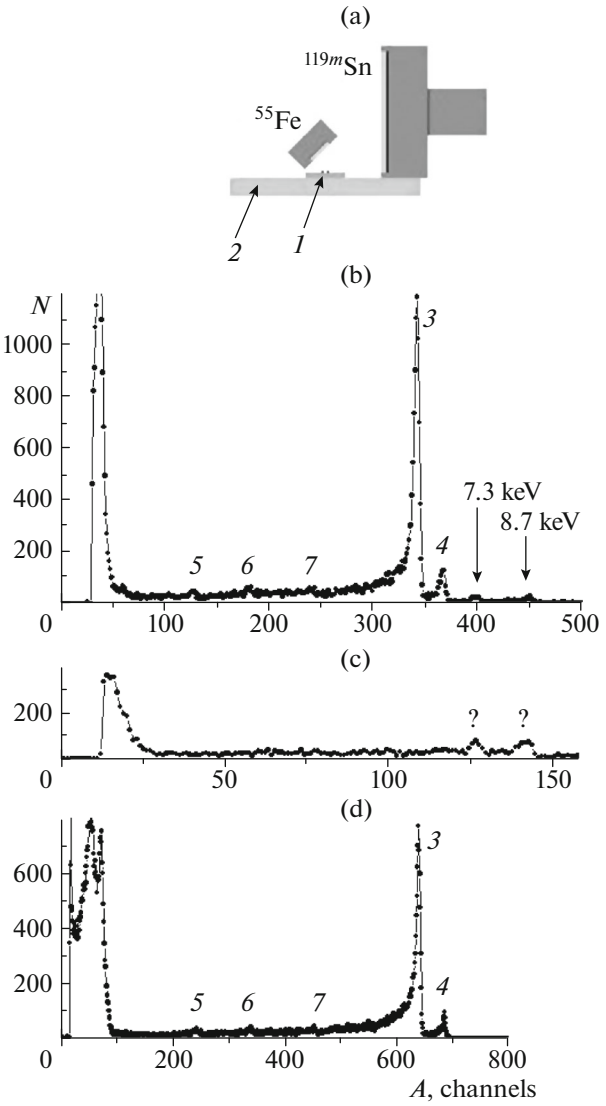

Fig. 1. (a) Schematic arrangement of the chip with detectors and the ^{119m}Sn and ^{55}Fe sources in the low-temperature chamber for experiments on calibrating the energy of the spectrum of the Mössbauer source. (b) Amplitude spectrum of the two sources, obtained with the 150 μm detector at $T = 1.38$ K and bias voltage $V_b = 0.786(3)$ mV on the detector; exposure time 26 min. (c) Amplitude spectrum of the ^{119m}Sn Mössbauer source radiation, obtained with the 150 μm detector at $T = 1.38$ K and bias voltage $V_b = 0.89$ mV on the detector; exposure time 26 min. (d) Amplitude spectrum of the ^{55}Fe source radiation, obtained with the 100 μm detector at $T = 1.39$ K and bias voltage $V_b = 0.808(2)$ mV on the detector; exposure time 13 min. A is the pulse amplitude, and N is the count in the channel. The numbers in the figures denote (*1*) the silicon chip with detectors; (*2*) the copper substrate attached to the cold finger of the low-temperature chamber; (*3*, *4*) the lines of MnK_α and MnK_β (energies, 5. 893 and 6.490 keV); (*5*, *6*) lines of the fluorescence of SiK_α (1.74 keV) and ClK_α (2. 622 keV); and (*7*) the escape peaks originating from niobium MnK_α and K_β (3.70 and 3.83 keV, respectively).

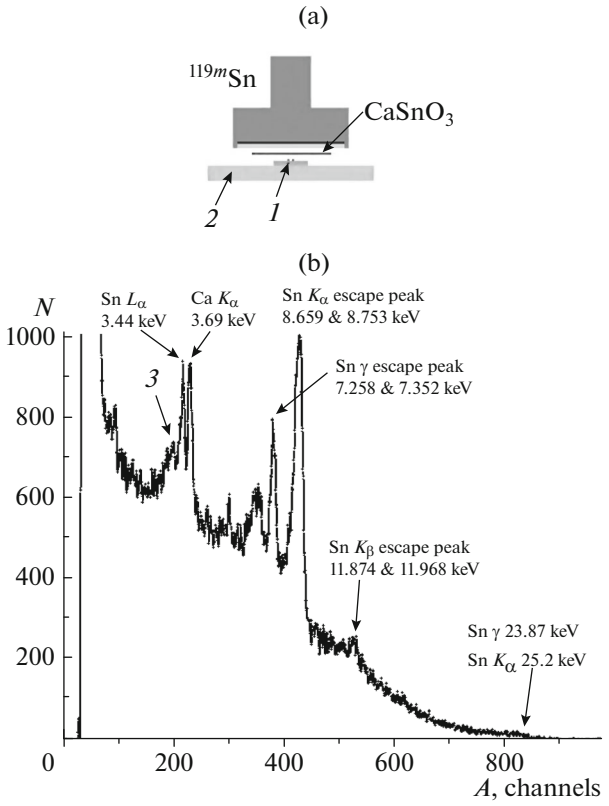

Fig. 2. (a) Schematic arrangement of the ^{119m}Sn source, the $CaSnO_3$ scatterer, and the chip with detectors in the low-temperature chamber. (b) Amplitude spectrum of the source radiation, obtained with 100 and 150 μm detectors at $T = 1.4$ K and bias voltage $V_b = 0.8$ mV on the detector; exposure time 7.28 h (32 spectra). A is the pulse amplitude, and N is the count in the channel. The numbers in the figures denote (*1*) the silicon chip with detectors; (*2*) the copper substrate attached to the cold finger of the low-temperature chamber; and (*3*) fluorescence line InL_α (3.29 keV).

characteristics are given in the Appendix to [4]. The STJs used as the detectors were squares with 100 and 150 μm sides (marked with 1 in Figs. 1a and 2a). The multilayer detectors had a Ti/Nb/Al/AlO_x/Al/Nb/NbN structure (30/100/8/1/13/150/30 nm thick, from bottom to top) and were made at the Kotel'nikov Institute of Radio Engineering and Electronics via photolithography and magnetron sputtering. The functioning of the detector's layers was described in [10]; the signal of the lower electrode was intentionally suppressed due to the asymmetric structure of the tunnel junction.

Measurements were made in a pumped glass helium cryostat at $T = 1.4$ K in the magnetic field of about 100 Oe required for the operation of the detectors and applied parallel to the plane of the tunnel junction along the diagonal of the square. The temperature was measured using a germanium thermometer. The chip with detectors and the source were on

the cold finger inside the low-temperature chamber created by the frame of the solenoid, which was immersed in liquid helium. For the rapid establishing of thermal equilibrium, and the stability of the detectors operation, the low-temperature chamber was filled with gaseous helium under the pressure at room temperature about 0.3 bar.

A charge-sensitive preamplifier operating at room temperature was used to register the pulses from the detectors. The same spectra registration system as in [3, 4] was used.

No diaphragms were used. The detectors were constantly exposed to direct radiation from the sources and scattered radiation.

RESULTS AND DISCUSSION

Our first experiment was conducted to calibrate the energy of the amplitude spectrum of the ^{119m}Sn source. A ^{55}Fe source emitting MnK_α and MnK_β X-ray radiation was added in the low-temperature chamber. The positions of the sources and the chip with the detectors are shown in Fig. 1a. The amplitude radiation spectrum of the two sources is shown in Fig. 1b. Figure 1c shows the probe spectrum of ^{119m}Sn separately, without the calibration source. The amplitude radiation spectrum of the ^{55}Fe source that we obtained earlier is presented in Fig. 1d. Numeric designations are given in the figure caption. A direct comparison of these spectra allows us to identify lines in the spectrum of the two sources, and to determine from the calibration curve [9, Fig. 4] the energy of the lines from the ^{119m}Sn source: 7.3 and 8.7 keV.

It should be noted that even though the activity of the ^{119m}Sn source exceeded the corresponding value of the ^{55}Fe source, the lines of the ^{119m}Sn source are notably weaker than those of the ^{55}Fe source, due to the great differences between the sizes of their active spots. We therefore needed to obtain a spectrum of much greater exposure to analyze the spectral lines of the ^{119m}Sn source. This was done by summing 32 corresponding spectra for the two detectors over 13 min, under the conditions of controlling the detectors bias voltage. The result is presented in Fig. 2b, and the scheme of the experiment is shown in Fig. 2a. The $CaSnO_3$ resonant scatterer was positioned between the source and the chip, allowing us to observe the Mössbauer effect at zero relative velocity of the source and detector. The pressure of the heat exchange gas in this experiment was quite low (it did not exceed ~0.01 bar at room temperature) so that the conversion electrons emitted from the scatterer could reach the detectors. However, an appropriate experiment with sufficient statistics without the scatterer for a direct comparison of the spectra with and without conversion electrons was not carried out. Because of this, the spectrum is not analyzed below from this point of view.

To analyze our data and identify the lines in the spectrum in Fig. 2b, we must focus a bit more on the initial stage of the complicated cascade of processes accompanying the absorption of radiation quantum in the detector absorber than is usual in describing superconducting tunnel detectors. In studying STJ detectors with Nb absorbers, the radiation is usually absorbed in the L shell of Nb. The energy of the Mössbauer radiation of the ^{119m}Sn source allows more detailed study of the features of absorption in *K* shell. Using the binding energies of the electrons in Nb (*see table*), we can determine the energies of photoelectrons for the *K* and *L* shells: $E^K = 4.887$ keV and $E^{L1} = 21.17$ keV. Holes in the K shell can be filled with electrons from the *L2* and *L3* shells with emission of Nb K_α radiation, which with Nb 150 nm thick is absorbed with a probability of 0.25%. In other words, the radiation almost completely escapes from the film. Thus the escape peak is formed. The energy remaining in the film is

$$E_{\text{escape peak}} = E_\gamma(\text{Sn}) - (E^K(\text{Nb}) - E^{L2,\,L3}(\text{Nb})) = E^K_{\text{photo}\,e} + E^{L2,\,L3} = 7.352,\ 7.258\ \text{keV}.$$

The probability of this process is around 75%. Holes in the *K* shell can also be filled by the emission of Auger electrons, the energies of which can be taken from tables or estimated with the example of *KL*1*L2* Auger electrons, using the formula [12]

$$E^{KLL}_{\text{Aug}\,e} = E^K(\text{Nb}) - E^{L2}(\text{Nb}) - E^{L1}(\text{Mo}) = 13.652\ \text{keV}.$$

Less probable processes are the holes in *K* shell being filled by electrons from *M*, *N*, and other shells. The remaining holes in *L* and higher shells are filled by the emission of Auger electrons, the upper limit on the energies of which is equal to the binding energy in an *L2* shell. A diagram of the processes that accompany the photoelectric effect is shown in Fig. 3.

It should be noted that the escape peak energies of Mössbauer radiation (7.352 and 7.258 keV) correlate well with the peak energy of 7.3 keV in Fig. 1b.

Performing similar calculations for the X-ray line of SnK_α, we obtain the energies of the respective escape peaks: 8.659 and 8.753 keV, which also correlate well with the peak energy of 8.7 keV in Fig. 1b.

The same lines can be seen in Fig. 2b. The escape peaks of SnK_β (11.874 and 11.968 keV) can also be identified in this figure. In addition, we observe the characteristic line of SnL_α (3.44 keV) and the fluorescence lines CaK_α (3.69 keV) and InL_α (3.29 keV, no. 3 in Fig. 2b). The Mössbauer line and the line of SnK_α are in the form of unresolved steps on the boundary of the spectrum to the right of the 800 channel. The other lines in the spectrum have yet to be identified.

Let us estimate ranges *R* for different electrons that accompany the photoelectric effect in niobium, using the Kanaya–Okayama formula [13]:

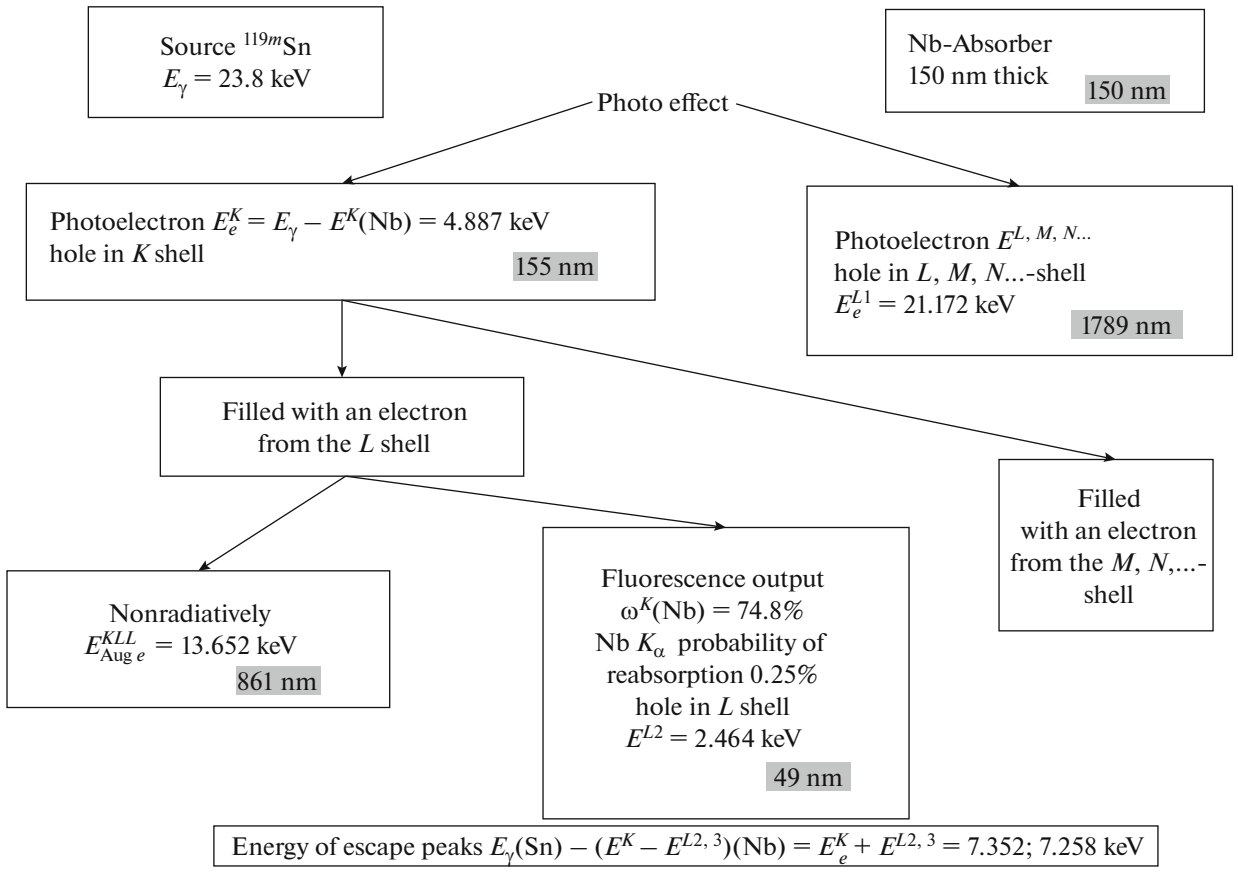

Fig. 3. Diagram of processes that accompany the photoelectric effect in the Nb-absorber of the detector. Range R of the electrons there is shown against the light grey background near their energies.

$$R[\mathrm{nm}] = \frac{27.6W}{\rho[\mathrm{g\ cm^{-3}}]Z^{0.89}}E^{1.67}\ [\mathrm{keV}],$$

where W is atomic weight, Z is atomic number, and ρ is density. Results for the ranges of electrons in niobium are presented in Fig. 3 in the form of the values in the rectangles against the grey background, next to the corresponding energies of the electrons using the example of the gamma line. As was shown in [14], electrons with ranges of $49 < 150$ nm participate in the formation of the peak of total absorption. For electrons with ranges of $155 \sim 150$ nm, the peak of incomplete absorption is formed. Electrons with ranges of $861 \gg 150$ nm transmit to the absorber only part of their energy, which apparently varies a great deal from event to event. As a result of these processes, well-defined escape peaks are formed, and the channel associated with the nonradiative relaxation of an excitation in an niobium atom does not result in a peak.

CONCLUSIONS

Despite the low efficiency of detecting Mössbauer radiation with the relatively high energy of 23.87 keV by a thin-film STJ detector based on niobium, we managed to register it and the associated X-ray emission by escape peaks with high energy resolution.

For a more complete interpretation of the spectrum, we must continue our work and repeat the experiment with a stronger source and a specially made scatterer.

Table 1. Binding energy of electrons for the different shells of niobium [11]

Shell	K	$L1$	$L2$	$L3$	$M1$	$M2$	$M3$	$M4$	$M5$	$N1$	$N2$	$N3$
Binding energy of an electron, eV	18983	2698	2465	2371	467	376	361	205	202	56.4	32.6	30.8

ACKNOWLEDGMENTS

The authors are grateful to S.K. Godovikov for his support in organizing this study.

REFERENCES

1. Andrianov, V.A., Kozin, M.G., Nefedov, L.V., Romashkina, I.L., Sergeev, S.A., and Shpinel, V.S., *Izv. Ross. Akad. Nauk, Ser. Fiz.*, 1996, vol. 60, no. 11, p. 184.
2. Kozin, M.G., Romashkina, I.L., Sergeev, S.A., Nefedov, L.V., Koshelets, V.P., and Filippenko, L.V., *Bull. Russ. Acad. Sci.: Phys.*, 2007, vol. 71, no. 9, p. 1302.
3. Kozin, M.G., Romashkina, I.L., Smirnova-Pinchukova, I.O., Koshelets, V.P., and Filippenko, L.V., *Bull. Russ. Acad. Sci.: Phys.*, 2015, vol. 79, no. 8, p. 1062.
4. Kozin, M.G., Romashkina, I.L., Filippenko, L.V., and Koshelets, V.P., *AIP Adv.*, 2016, vol. 6, p. 025315.
5. Belozerskii, G.N., *Messbauerovskaya spektroskopiya kak metod issledovaniya poverkhnosti* (Mössbauer Spectroscopy as a Surface Analysis Technique), Moscow: Energoatomizdat, 1990.
6. Nomura, K., Ujihira, Y., and Vertes, A., *J. Radioanal. Nucl. Chem.*, 1996, vol. 202, nos. 1–2, p. 103.
7. Isozumi, Y., Ito, S., Fujii, T., and Katano, R., *Rev. Sci. Instrum.*, 1989, vol. 60, p. 3262.
8. Sawicki, J.A., *Nucl. Instrum. Methods Phys. Res., Sect. B*, 1986, vol. 16, p. 483.
9. Kozin, M.G., Romashkina, I.L., Sergeev, S.A., Nefedov, L.V., Koshelets, V.P., and Filippenko, L.V., *Instrum. Exp. Tech.*, 2006, vol. 49, no. 6, p. 868.
10. Kozin, M.G., Romashkina, I.L., Sergeev, S.A., et al., *Nucl. Instrum. Methods Phys. Res., Sect. A*, 2004, vol. 520, nos. 1–3, p. 250.
11. http://henke.lbl.gov/.
12. Pavlinskii, G.V., *Osnovy fiziki rentgenovskogo izlucheniya* (Basics of X-Ray Radiation Physics), Moscow: Fizmatlit, 2007.
13. Lukiyanov, F.A., Rau, E.I., and Sennov, R.A., *Bull. Russ. Acad. Sci.: Phys.*, 2009, vol. 73, no. 4, p. 441.
14. Kozin, M.G. and Romashkina, I.L., *Bull. Russ. Acad. Sci. Phys.*, 2012, vol. 76, no. 10, p. 1061.

Translated by N. Petrov